AVIAN DISEASES 59:410–418, 2015

Histopathologic and Myogenic Gene Expression Changes Associated with Wooden Breast in Broiler Breast Muscles

Sandra G. Velleman,[A] and Daniel L. Clark

Department of Animal Sciences, Ohio Agricultural Research and Development Center, The Ohio State University, Wooster, OH 44691

Received 20 April 2015; Accepted 20 May 2015; Published ahead of print 21 May 2015

SUMMARY. The wooden breast condition is a myopathy affecting the pectoralis major (p. major) muscle in fast-growing commercial broiler lines. Currently, wooden breast–affected birds are phenotypically detected by palpation of the breast area, with affected birds having a very hard p. major muscle that is of lower value. The objective of this study was to compare the wooden breast myopathy in two fast-growing broiler lines (Lines A and B) with incidence of wooden breast to a slower growing broiler Line C with no phenotypically observable wooden breast. One of the characteristics of the wooden breast condition is fibrosis of the p. major muscle. Morphologic assessment of Lines A and B showed significant fibrosis in both lines, but the collagen distribution and arrangement of the collagen fibrils was different. In Line A, the collagen fibrils were tightly packed, whereas in Line B the collagen fibrils were diffuse. This difference in collagen organization may be due to the expression of the extracellular matrix proteoglycan decorin. Decorin is a regulator of collagen crosslinking and is expressed at significantly higher levels in Line A wooden breast–affected p. major muscle, which would lead to tightly packed collagen fibers due to high levels of collagen crosslinking. Furthermore, expression of the muscle-specific transcriptional regulatory factors for proliferation and differentiation of muscle cells leading to the regeneration of muscle in response to muscle damage was significantly elevated in Line A, and only the factor for differentiation, myogenin, was increased in Line B. The results from this study provide initial evidence that the etiology of the wooden breast myopathy may vary between fast-growing commercial broiler lines.

RESUMEN. Cambios histopatológicos y expresión genética miogénica asociados con miopatía tipo ''pechuga de madera'' en los músculos de la pechuga de pollos de engorde.

La condición en los músculos de la pechuga tipo ''pechuga de madera'' es una miopatía que afecta al músculo pectoral mayor (*pectoralis major*) en las líneas de pollos de engorde comerciales de rápido crecimiento. En la actualidad, las aves afectadas con ''pechuga de madera'' son detectadas fenotípicamente mediante palpación de la zona del pecho, las aves afectadas tienen un músculo *p. major* muy duro que es de inferior valor comercial. El objetivo de este estudio fue comparar la miopatía tipo ''pechuga de madera'' en dos líneas de pollos de engorde de crecimiento rápido (líneas A y B) con incidencia para ''pechuga de madera'' en comparación con una línea de pollo de engorde de crecimiento lento, Línea C sin ''pechuga de madera'' fenotípicamente observable. Una de las características de la condición ''pechuga de madera'' es la fibrosis del músculo *p. major*. La evaluación morfológica de las líneas A y B mostró fibrosis significativa en ambas líneas, pero la distribución y distribución de las fibras de colágena era diferente. En la Línea A, las fibras de colágena estaban densamente empaquetadas, mientras que en la línea B las fibras de colágena eran difusas. Esta diferencia en la organización de la colágena puede ser debida a la expresión del proteoglicano llamado decorina, de la matriz extracelular. La decorina es un regulador del entrecruzamiento de colágeno y se expresó en niveles significativamente más altos en la línea A con el músculo *p. major* afectado por ''pechuga de madera'', lo que provocaría que las fibras de colágeno se empacaran densamente debido a los altos niveles de entrecruzamiento de la colágena. Además, la expresión de los factores reguladores de la transcripción específicos del músculo para la proliferación y diferenciación de las células musculares, que conducen a la regeneración del músculo en respuesta a un daño muscular fue significativamente elevado en la línea A, y sólo el factor de diferenciación, miogenina, se incrementó en la línea B. Los resultados de este estudio proporcionan evidencia inicial de que la etiología de la miopatía de ''pechuga de madera'' puede variar entre las líneas de pollos de engorde comerciales de rápido crecimiento.

Key words: broilers, collagen, muscle, myopathy, satellite cell, wooden breast

Abbreviations: EGFR = epidermal growth factor receptor; GAPDH = glyceraldehyde-3-phosphate dehydrogenase; HP = hydroxylsylpridinoline; MYOD1 = myogenic determination factor 1; p. major = pectoralis major; qPCR = quantitative PCR

The worldwide broiler industry has recently been faced with emerging myopathies affecting the pectoralis major (p. major) muscle phenotypic appearance and meat quality. One of these myopathies, ''wooden breast,'' results in a hard p. major muscle that is of lower value. Because the p. major muscle, or breast muscle, is economically the most valuable part of the broiler carcass in the United States (31), the wooden breast condition results in considerable economic losses to the industry. The phenotypic hardness of the p. major muscle in wooden breast–affected birds is associated with the p. major muscle being pale and often having a white-striped appearance (17,23,29). Furthermore, the wooden breast myopathy to date has only been reported in the p. major muscle in predominantly fast-growing broiler lines (Sihvo et al., 2013).

Meat quality is the direct result of muscle morphologic structure and cellular biologic processes regulating muscle development and growth. The poultry industry has made substantial genetic improvements in growth rate and breast meat yield. However, these increases have changed both the morphometry and cell biology of the p. major muscle. In general, growth selection has resulted in larger diameter muscle fibers (9), decreased capillary blood supply to the muscle (30), reduced connective tissue spacing between muscle fiber bundles and muscle fibers (9,30), and increased myofiber degeneration (38). These types of changes result from a shift in muscle growth toward posthatch muscle fiber hypertrophy mediated

[A]Corresponding author. E-mail: velleman.1@osu.edu

by the adult myoblast, satellite cell, population of cells. Fast-growing male meat-type chickens have p. major muscle fibers three to five times wider than slower growing birds (9).

Muscle growth is a precisely regulated process that has distinct embryonic and posthatch phases. Early embryonic development of skeletal muscle results from the proliferation, differentiation, and fusion of embryonic myoblasts within newly formed muscle beds. Muscle fiber formation is essentially complete at hatch; however, a large increase in muscle DNA content occurs after hatch. Posthatch muscle development is largely due to the activity of muscle satellite cells associated with existing muscle fibers. Satellite cells are located between the basement membrane and plasmalemma of muscle fibers (20). The satellite cells proliferate, differentiate, and fuse with adjacent fibers (22). The additional muscle fiber nuclei derived from satellite cells ultimately lead to increased muscle mass through increased protein synthesis, resulting in muscle fiber enlargement or hypertrophy (1). Skeletal muscle nuclei at hatch consist of a high percentage of proliferating satellite cells. At the end of the growth phase, the number of satellite cells decreases to less than 5% of total myofiber nuclei and become largely quiescent (11). Satellite cells will re-enter the cell cycle in response to damage and regenerate the muscle fiber. Upon being activated the satellite cell will express muscle-specific transcriptional regulatory factors in a sequential pattern, with myogenic determination factor 1 (MYOD1) being expressed in proliferating cells, followed by myogenin expression as the cells enter differentiation (5,6,15,39).

Satellite cell proliferation and differentiation are also, in part, regulated by the extrinsic extracellular matrix environment. One function of the extracellular matrix is to mediate the cellular response to certain growth factors that can either stimulate or inhibit satellite cell proliferation and differentiation. Decorin is a multifunctional small leucine-rich proteoglycan located in the extracellular matrix of skeletal muscle. The decorin central core protein binds to the growth factors transforming growth factor-β (TGF-β) and myostatin (4,28). Both of these growth factors are strong inhibitors of satellite cell proliferation and differentiation. Decorin can sequester both TGF-β and myostatin from their receptors, preventing these growth factors from inhibiting proliferation and differentiation. Decorin is a regulator of collagen fibrillogenesis by mediating collagen crosslinking (13,37). Thus, decorin can regulate cell growth and organization of the extracellular matrix. Skeletal muscle fibrosis has been reported to be associated with the expression of decorin, TGF-β, and myostatin (40), which also may be associated with the fibrosis observed in the wooden breast myopathy.

To date, there are no published reports comparing the morphology and cell biology in fast-growing broiler lines with reported incidence of wooden breast. Currently, the wooden breast myopathy is limited to a phenotypic description of a nonpliable or hard breast muscle. Thus, the first objective of the current study was to compare morphology of the wooden breast condition in two fast-growing commercial broiler lines with phenotypic detection of wooden breast to determine whether all wooden breast muscle has a similar p. major muscle morphologic structure. The second objective of this study was to begin to establish the cellular mechanism involved in wooden breast necrosis and the ability of the muscle fibers to regenerate after degeneration.

MATERIALS AND METHODS

Birds. Males from three commercial broiler lines (A, B, and C) were used to obtain p. major samples for histology and gene expression analysis at the time of processing (approximately 40 days of age) by a commercial producer. Lines A and B were fast-growing broiler lines with incidence of the wooden breast myopathy. Line C was a slower growing broiler line with no phenotypically detectable wooden breast. In total, 81 birds were used in the current study, with Line A containing 61 birds, Line B containing 7 birds, and Line C containing 20 birds. The birds used in this study were selected at random by personnel for the commercial producer. Phenotypic presence of wooden breast was determined by experienced producer personnel that palpated the p. major muscle of the live bird. Immediately after processing, histology and tissue samples were removed and sent to S.G.V.'s lab for RNA analysis and further processing.

Histology. Immediately after the birds were euthanized, the skin was removed from the breast region and a sample of the p. major muscle was removed for histology. The sample was obtained by carefully dissecting approximately 0.5 cm of the muscle fibers along the orientation of the muscle fibers for a length of 3 cm. The ends of the muscle sample were tied to wooden applicator sticks by using surgical thread before removal to prevent muscle contractions. The samples were processed as described in Jarrold et al. (14). The resulting paraffin blocks were cross-sectioned at 5 μm and mounted on Starfrost Adhesive slides (Mercedes Medical, Sarasota, FL). Overall muscle morphology was evaluated by staining with hematoxylin and eosin as described in Velleman and Nestor (35). Masson Trichrome staining was done to detect connective tissue, especially collagen, in the perimysial and endomysial connective tissue layers. The Accustain Trichrome Stain Kit (Sigma-Aldrich, St. Louis, MO) was used according to the manufacturer's directions along with a hematoxylin counterstain. Detection of connective tissue proteoglycans with attached glycosaminoglycans was accomplished with an Alcian blue stain and a nuclear fast red counterstain. Alcian blue solution contained 1% Alcian blue 8GX (Eastman Kodak Co., Rochester, NY) in 3% glacial acetic acid. After staining the samples for 30 min in Alcian blue solution, the slides were rinsed with water and counterstained for 5 min with 0.1% nuclear fast red solution: 0.1 g of nuclear fast red (Sigma-Aldrich), 5 g of aluminium sulfate (Thermo Fisher Scientific, Pittsburgh, PA), and distilled water to 100 ml.

The stained sections were analyzed for muscle morphology with an IX70 fluorescent microscope (Olympus America, Melville, NY) and QImaging digital camera (QImaging, Burnaby, BC, Canada) equipped with CellSens Imaging software (Olympus America). Each slide from each bird contained a minimum of four sections, and five fields from each section were evaluated for fiber necrosis, fibrosis, macrophage infiltration, collagen content, and proteoglycan content. A score of 1 was given to samples with no abnormalities and a score of 5 was given to samples with extensive defects. For fiber necrosis, a score of 1 represented no necrosis and a score of 5 represented extensive necrosis, with scores of 2–4 being intermediate. For fibrosis, a score of 1 represented no replacement of muscle fibers with connective tissue and a score of 5 represented extensive fibrosis, with scores of 2–4 being intermediate. For macrophage infiltration, a score of 1 represented no infiltration of macrophages and score of 5 represented extensive infiltration, with scores of 2–4 being intermediate. Collagen content was scored as an additional measure of fibrosis, with a score of 1 representing no additional collagen deposition in the connective tissue spaces and a score of 5 representing extensive collagen deposition, with scores of 2–4 being intermediate. A composite wooden breast score was calculated to identify the severity of the wooden breast condition by adding the histologic fiber necrosis score, fibrosis score, macrophage infiltration score, and collagen content score.

Total RNA extraction and cDNA synthesis. Immediately after the birds were euthanized, the skin was removed from the breast region and a sample of the p. major muscle was removed for RNA by carefully dissecting the p. major muscle and placing the sample in RNAlater (Ambion, Grand Island, NY). The p. major muscle sample from each bird was extracted for total RNA by using RNAzol (Molecular Research Center, Cincinnati, OH) according to the manufacturer's protocol. The cDNA was synthesized using Moloney murine leukemia virus (MMLV) reverse transcriptase (Promega, Madison, WI). The reaction consisted of 0.5 μg of total RNA, 1 μl of 50 μM oligo$(dT)_{20}$ (Operon, Huntsville,

Table 1. SYBR Green real-time qPCR primer sequences.

	Forward primer	Reverse primer	Amplicon (bp) size	Accession no.
MYOD1	5′-GACGGCATGATGGAGTACAG-3′	5′-AGCTTCAGCTGGAGGCAGTA-3′	201	NM_204214.2
Myogenin	5′-GGCTTTGGAGGAGAAGGACT-3′	5′-CAGAGTGCTGCGTTTCAGAG-3′	184	NM_204184.1
Decorin	5′-AAGGTTCTGCCTGGAGTTGA-3′	5′-TTGGCACTCTTTCCAGACCT-3′	254	NM_001030747.2
Myostatin	5′-AAACGGTCCCGCAGAGATTT-3′	5′-CAGGTGAGTGTGCGGGTATT-3′	195	NM_00100146.1
TGF-β	5′-AGGATCTGCAGTGGAAGTGG-3′	5′-AGGCCCACGTAGTAAAATGAT-3′	300	JQ423909.1

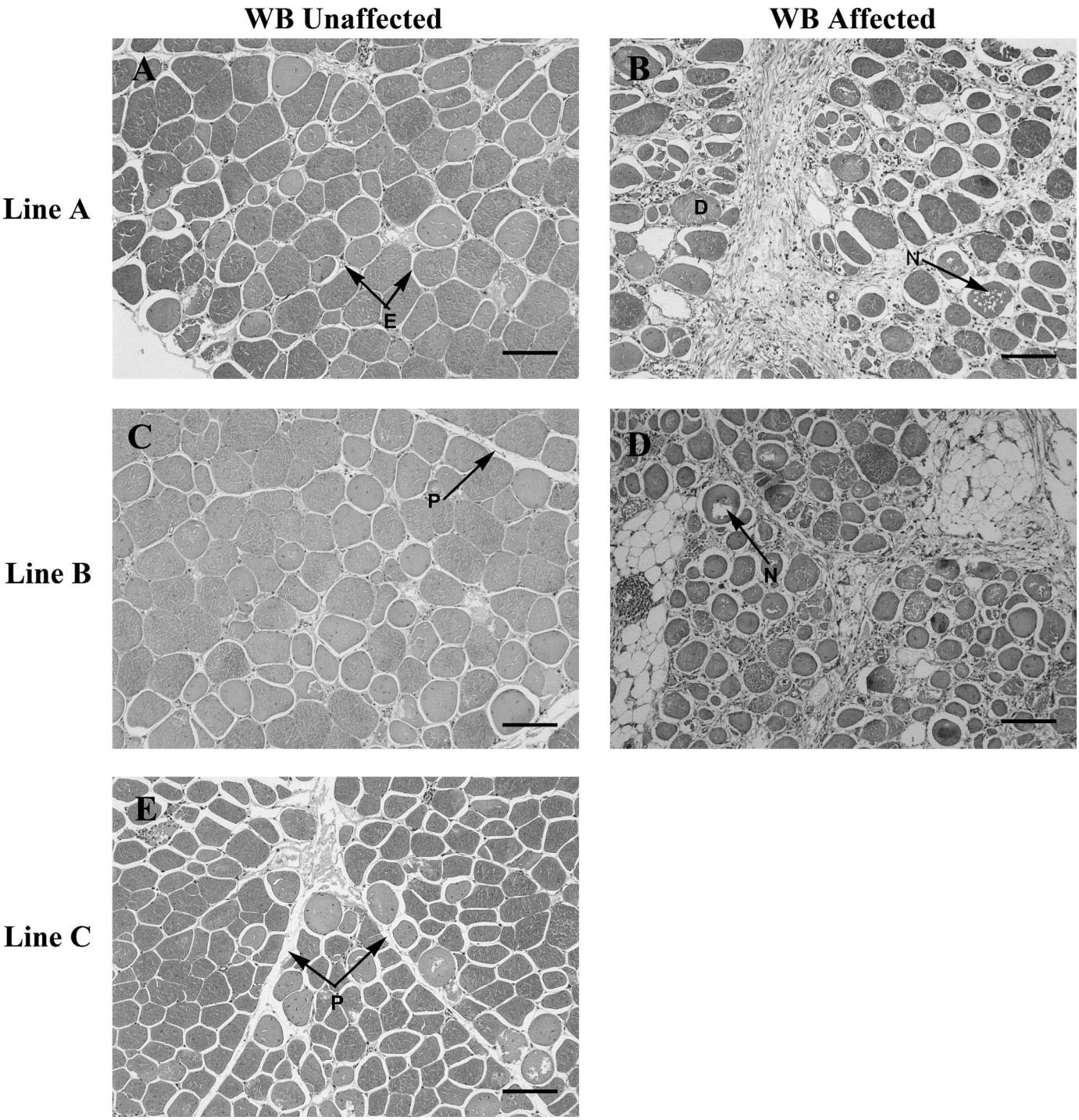

Fig. 1. Morphologic structure in wooden breast–affected and –unaffected p. major muscle. A, C, and E are representative images of wooden breast–unaffected p. major muscles from Line A, B, and C, respectively. B and D are representative images of wooden breast–affected p. major muscles from Line A and B, respectively. D = degenerating muscle fiber; E = endomysial connective tissue space; N = fiber necrosis; P = perimysial connective tissue space; WB = wooden breast. Bar = 100 μm.

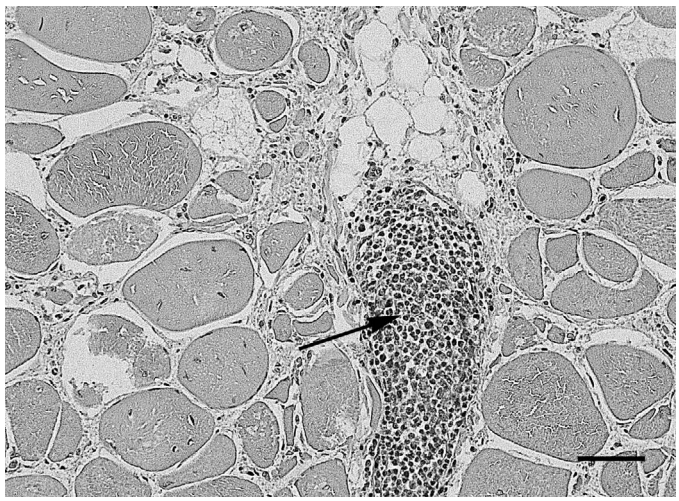

Fig. 2. Macrophage infiltration associated with the wooden breast myopathy. The arrow highlights the macrophages. Bar = 50 μm.

AL), and nuclease-free water up to 13.5 μl; this mixture was incubated at 80 C for 5 min and then cooled on ice. After cooling, 11.5 μl of the reaction mixture, 5 μl of MMLV reverse transcriptase 5× buffer (Promega), 1 μl of 10 mM deoxynucleoside triphosphate mix, 0.25 μl of RNasin (40 U/μl), 1 μl of MMLV (200 U/μl), and 4.25 μl of nuclease-free water were added. The total 25 μl reaction mixture was incubated at 55 C for 60 min and then heated at 90 C for 10 min to stop the reaction. After the cDNA synthesis, 25 μl of nuclease-free water was added to the cDNA.

Real-time quantitative PCR (qPCR). qPCR was performed using the DyNAmo Hot Start SYBR Green qPCR kit (Thermo Fisher Scientific) with a DNA Engine Opticon 2 real-time system (Bio-Rad Laboratories, Hercules, CA). Each PCR reaction consisted of 2 μl of cDNA, 10 μl of 2× master mix, 1 μl of 10 μM primer mixture (forward and reverse) of the target genes (Table 1), and 7.0 μl of nuclease-free water for a 20-μl reaction volume. The specificity of the gene-specific primers was confirmed by DNA sequencing of the amplified sequence product (Molecular and Cellular Imaging Center, Ohio Agricultural Research and Development Center, The Ohio State University, Wooster, OH). The qPCR was performed with the following conditions for MYOD1 and myogenin: denaturation (94 C for 15 min), amplification and quantification (35 cycles of 94 C for 30 sec, 58 C for 30 sec, and 72 C for 30 sec), and final extension at 72 C for 5 min. Glyceraldehyde-3-phosphate dehydrogenase (GAPDH), decorin, myostatin, and TGF-β were amplified under the following conditions: denaturation (94 C for 15 min), amplification and quantification (35 cycles of 94 C for 30 sec, 55 C for 30 sec, and 72 C for 30 sec), and final extension at 72°C for 5 min. The melting curve program was 52 C to 95 C, 0.2 C/read, and a 1-sec hold. The relative level of gene expression was calculated using the standard curve for each target gene as described previously by Liu et al. (18). Standard curves were constructed using serial dilutions of the purified PCR products of each gene in Table 1. The amount of sample cDNA for each gene was interpolated from the corresponding standard curve. All of the sample concentrations fell within the values of the standard curves. This normalization was calculated as an arbitrary unit based on the GAPDH concentration. To reduce plate-to-plate variation, all samples were standardized to the Line C samples by calculating the mean of the Line C samples for each plate and then obtaining a standardization ratio by dividing the mean of the Line C samples for each plate by the mean of the Line C samples across all plates. The standardization ratio was then used to normalize across plates. Randomly selected samples from all qPCR reactions were resolved by agarose gel electrophoresis to ensure gene amplification specificity. A negative control, a well with no template, was included in each PCR reaction to detect possible contamination. For qPCR analysis, all samples were run in triplicate, and values were averaged to obtain the mean expression for each sample.

Statistical analysis. For gene expression analysis, the samples were categorized as either wooden breast affected or wooden breast unaffected by histologic evaluation. Due to the unequal representation of treatments, the samples were divided into five treatment categories: Line A, wooden breast affected; Line A, wooden breast unaffected; Line B, wooden breast affected; Line B, wooden breast unaffected; and Line C, wooden breast unaffected. The treatment combinations were analyzed individually, and the GLIMMIX procedure of SAS (SAS Institute, Inc., Cary, NC) was used to separate the means. Differences were considered significant at $P < 0.05$. For the correlation of gene expression with histologic evaluation, the three lines were compiled, and Pearson correlation coefficients were obtained using the CORR procedure of SAS.

RESULTS

Histologic assessment of the wooden breast myopathy. Overall morphologic assessment (Fig. 1) showed the Lines A and B wooden breast–affected p. major muscle (Fig. 1A, B) lacked muscle fiber bundle organization, including well-defined perimysial and endomysial connective tissue spacing. Average myofiber diameter in the wooden breast–affected p. major muscles were smaller in Lines A and B compared to the unaffected samples. Lines A and B wooden breast muscle fibers had diameters of 46.2 ± 1.97 and 41.6 ± 1.32 μm compared to the unaffected muscle fibers, with diameters of 75.1 ± 2.19 and 74.4 ± 2.04 μm, respectively. Line C, a slower growing broiler line without incidence of wooden breast, had an average myofiber diameter of 56.2 ± 1.20 μm. Extensive myofiber lysis and degeneration were present in the wooden breast–affected p. major muscles compared to the unaffected p. major muscles. In addition, in areas of severe degeneration, infiltration of macrophages were present (Fig. 2). Extracellular matrix glycosaminoglycans covalently attached to proteoglycan core proteins have a very high negative charge and ionically interact with water. Increases in

Table 2. Gene expression analysis of three genetic lines affected or unaffected by the wooden breast (WB) morphology.[A]

	Line A		Line B		Line C
	WB affected	WB unaffected	WB affected	WB unaffected	WB unaffected
n[B]	42	19	5	2	20
MYOD1	16.3 ± 0.8a	7.3 ± 1.2bc	12.1 ± 2.3ab	10.9 ± 3.6abc	6.0 ± 1.1c
Myogenin	19.4 ± 1.4a	2.7 ± 2.1b	19.7 ± 4.0a	3.6 ± 6.3b	1.4 ± 2.0b
Decorin	43.1 ± 2.8a	6.6 ± 4.2c	25.8 ± 8.2b	3.9 ± 13.0bc	1.6 ± 4.1c
Myostatin	22.7 ± 1.5a	12.0 ± 2.2b	16.2 ± 4.3ab	16.1 ± 6.8ab	7.3 ± 2.1b
TGF-β	5.4 ± 0.3a	2.3 ± 0.5bc	4.2 ± 1.0ab	1.6 ± 1.5bc	1.2 ± 0.5c

[A]Means of arbitrary units ± SEM within a row and with a different lowercase letters are significantly different ($P < 0.05$).
[B]Number of animals within each category.

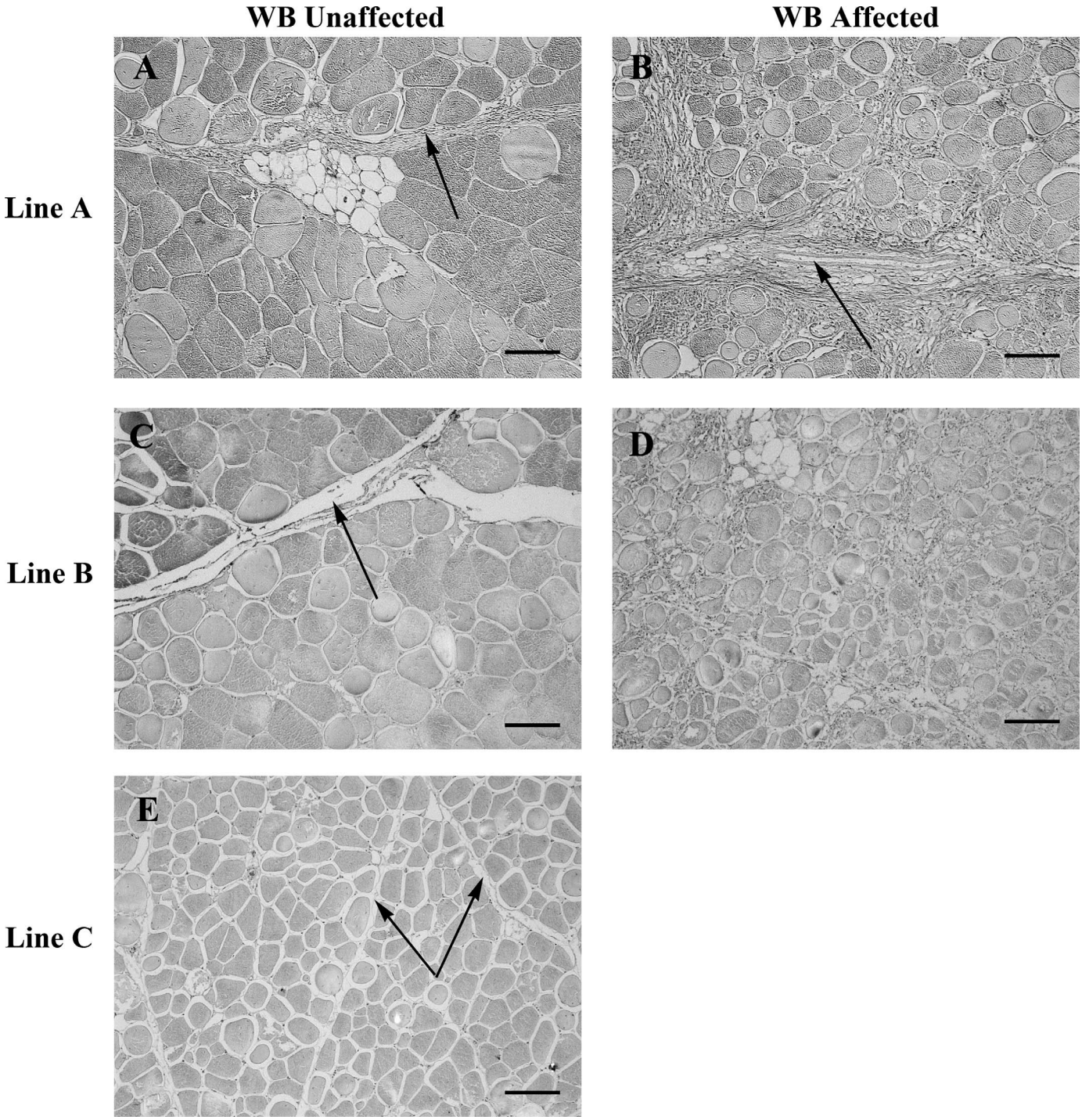

Fig. 3. Detection of connective tissue glycosaminoglycans by Alcian blue staining in wooden breast–affected and –unaffected p. major muscle. A, C, and E are representative images of wooden breast–unaffected p. major muscles from Line A, B, and C, respectively. B and D are representative images of wooden breast–affected p. major muscle from Line A and B, respectively. The arrows highlight perimysial connective tissue spacing. WB = wooden breast. Bar = 100 μm.

glycosaminoglycan content would change water-holding capacity of the muscle. Alcian blue staining was used to detect glycosaminoglycans attached to proteoglycan core proteins showed no observable change in connective tissue glycosaminoglycan content in wooden breast–affected p. major muscles in either Line A or B compared to the unaffected p. major muscles and Line C (Fig. 3). Wooden breast–affected p. major muscle in Lines A and B both contained extensive fibrosis. Masson's trichrome staining showed extensive extracellular collagen deposition in both Lines A and B, when the wooden breast myopathy is present, compared to the unaffected samples and Line C (Fig. 4). The distribution of extracellular collagen was different between Lines A and B. Line A exhibited a dense parallel arrangement of collagen fibers, whereas Line B had diffuse and variable distribution of collagen.

Expression of MYOD1, myogenin, decorin, TGF-β, and myostatin. The expression of MYOD1, myogenin, decorin,

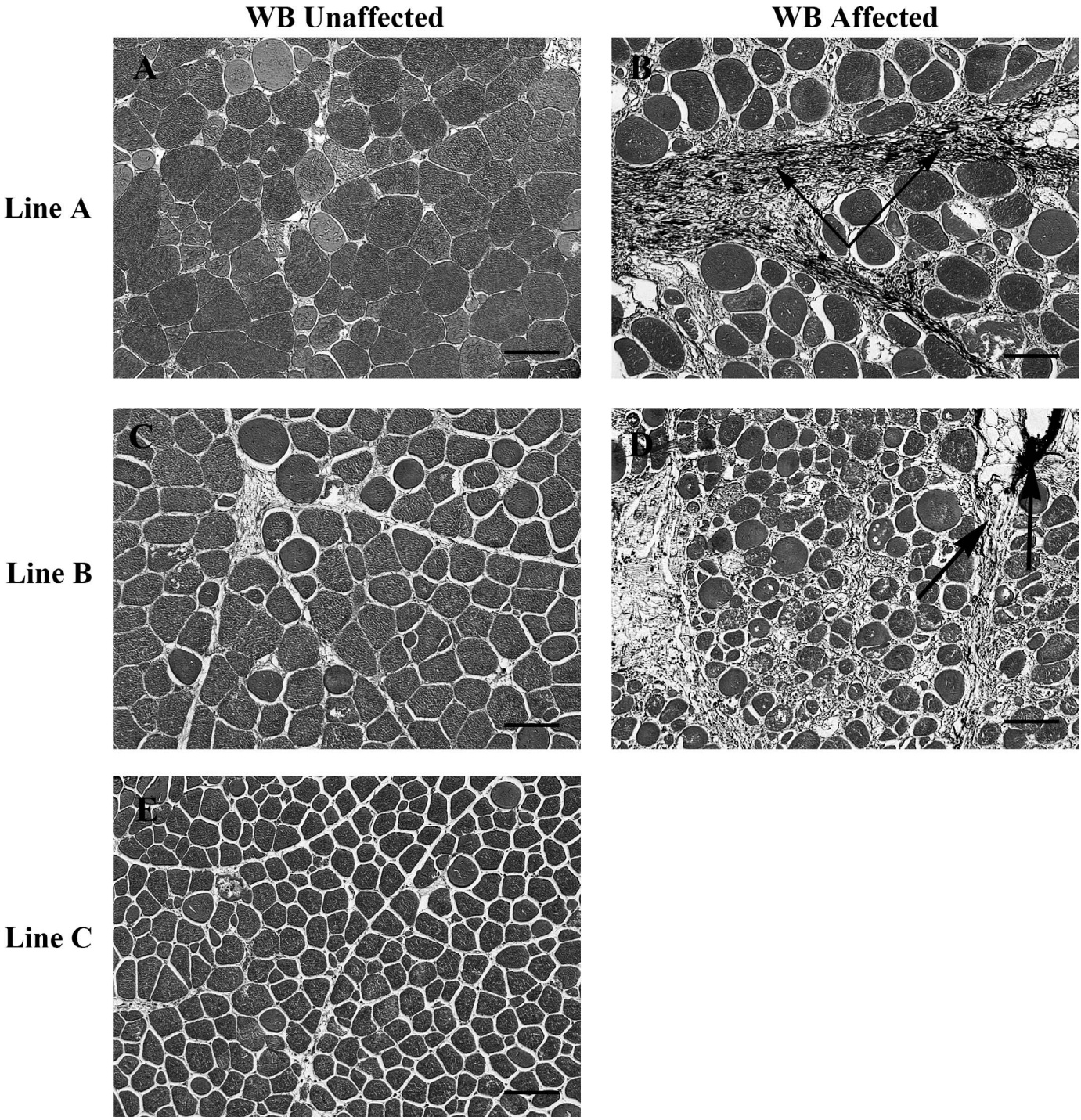

Fig. 4. Detection of collagen by Masson's trichrome staining in wooden breast–affected and –unaffected p. major muscle. A, C, and E are representative images of wooden breast–unaffected p. major muscle from Line A, B, and C, respectively. B and D are representative images of wooden breast–affected p. major muscle from Line A and B, respectively. The arrows highlight collagen staining in the perimysial connective tissue space. WB = wooden breast. Bar = 100 μm.

TGF-β, and myostatin was measured in wooden breast–affected and –unaffected p. major muscles from Lines A and B, and C, respectively (Table 2). As shown in Table 2, the wooden breast myopathy in the Line A results in increased MYOD1, myogenin, decorin, TGF-β, and myostatin expression compared to the unaffected samples in Lines A and C. In contrast to Line A, Line B wooden breast–affected p. major muscles only had a significant increase in myogenin expression compared to the unaffected Line B samples. Decorin expression was approximately 40% lower in Line B compared to Line A wooden breast–affected p. major muscles. All the genes assayed except myostatin were significantly higher in the Line B wooden breast–affected p. major muscles compared to Line C. Correlation coefficient analysis combining the histologic analysis with the expression for each gene showed that the genes studied were all significantly correlated with the wooden breast myopathy. However, decorin, MYOD1, and myogenin had the

Table 3. Correlation coefficients for histomorphologic characteristics and gene expression.

	Fiber necrosis	Fibrosis	Macrophage infiltration	Collagen content	Proteoglycan content	Composite WB score[A]
MYOD1						
Pearson[B]	0.54	0.72	0.73	0.65	0.61	0.73
P[C]	<0.001	<0.001	<0.001	<0.001	<0.001	<0.001
Myogenin						
Pearson	0.47	0.75	0.73	0.69	0.65	0.73
P	<0.001	<0.001	<0.001	<0.001	<0.001	<0.001
Decorin						
Pearson	0.49	0.78	0.76	0.74	0.62	0.77
P	<0.001	<0.001	<0.001	<0.001	<0.001	<0.001
Myostatin						
Pearson	0.27	0.53	0.53	0.50	0.39	0.52
P	0.01	<0.001	<0.001	<0.001	<0.01	<0.001
TGF-β						
Pearson	0.42	0.68	0.70	0.65	0.58	0.68
P	<0.001	<0.001	<0.001	<0.001	<0.001	<0.001

[A]Composite WB score = fiber necrosis score + fibrosis score + macrophage infiltration score + collagen content score.
[B]Pearson correlation coefficient for the comparison of each histomorphologic score and gene.
[C]*P* value for each Pearson correlation coefficient.

greatest correlation with the composite wooden breast score across all samples from each line (Table 3).

DISCUSSION

In rapidly growing birds, more muscle fiber fragmentation and reduced endomysial and perimysial connective tissue spacing are present in the p. major muscle (31,38). The p. major muscle is a fast twitch anaerobic muscle composed primarily of fast twitch glycolytic (type IIb) muscle fibers (2,3,19). Lactic acid is produced by anaerobic respiration present in glycolytic muscle and is removed by the circulatory system. Sosnicki and Wilson (30) reported a reduction in the number of capillaries surrounding degenerating or necrotic areas. With growth-selected birds, the p. major muscle frequently has reduced endomysial and perimysial connective tissue spacing (32,38), thereby limiting the available space for capillaries and hence reducing the amount of lactic acid removed from the muscle. In the case of p. major myopathies such as wooden breast, it is probable that lactic acid produced from the anaerobic respiration is not efficiently removed, resulting in a decrease in pH, muscle damage, and satellite cell–mediated regeneration. In addition, p. major muscles with the wooden breast myopathy have a high proportion of necrotic or hypercontracted myofibers.

Satellite cell–mediated repair of muscle fiber damage. Activation of satellite cell regeneration mechanisms to repair damaged muscle fibers will stimulate both proliferation and differentiation and result in the expression of the myogenic transcriptional regulatory factors. For Line A, both MYOD1 and myogenin were expressed at significantly higher levels in the wooden breast–affected p. major muscles, whereas in Line B only myogenin expression was higher in the affected p. major muscles. It is possible that MYOD1 expression was affected at a time not measured as the expression data represent the amount of MYOD1 present at the time of processing. However, the data for the muscle transcriptional regulatory factors do support that satellite cell–mediated regeneration is occurring in p. major muscle with the wooden breast myopathy.

Despite the regeneration mechanisms being activated, muscle fiber diameter is smaller in the wooden breast–affected p. major muscles in both Lines A and B. Regeneration should not reduce myofiber diameter. Expression levels of the growth factors TGF-β and myostatin were measured as both interact with decorin and function in decorin-mediated mechanisms regulating cell growth (4). The wooden breast condition in Line A had significantly higher levels of TGF-β and myostatin, whereas in Line B changes in TGF-β and myostatin expression were not significant. Because TGF-β and myostatin are strong inhibitors of muscle cell proliferation and differentiation, reduced myofiber fiber diameter in Line A wooden breast samples is likely, in part, to be due to elevated growth factor expression suppressing satellite cell–mediated repair. However, growth factor repression of muscle fiber regeneration is probably not the only mechanism inhibiting cell growth as Line B also has decreased muscle fiber size compared to the unaffected and Line C muscle fiber diameters. A prime candidate for regulating satellite cell–mediated regeneration is decorin.

Decorin expression and collagen organization. Decorin regulates cell growth by binding to and activating the epidermal growth factor receptor (EGFR) (27). When decorin binds to and activates EGFR, it induces growth inhibition through an upregulation of cyclin-dependent kinase inhibitor $p21^{WAF1}$ expression (8,13,21). This pathway of decorin regulation of cell growth has been shown to play a significant role in tumor progression. In many tumor types, decorin levels are either lost or reduced (10,12,16). Increasing decorin levels through exogenous delivery to the tumor either slows or eliminates tumorigenic cell growth (24,25). Although decorin regulation of EGFR has not been shown in muscle regeneration to date, in fibrotic muscle elevated levels of decorin may inhibit satellite cell–mediated growth through activating EGFR.

Although both Lines A and B in the current study exhibited fibrosis, the fibrotic changes were distinct between the two lines in terms of the extracellular distribution of collagen fibers surrounding the cells. Line A was characterized by extensive parallel packing of the collagen fibers, whereas Line B had a diffuse distribution of collagen. Parallel packing of collagen is due to extensive crosslinking of the collagen fibrils (33,34) that will result in the Line A p. major muscle being harder than that of Line B. Wooden breast in the processing plant is detected by visual observance and by palpation. Even among birds that were phenotypically identified as normal in Line B, approximately 70% showed some evidence of muscle damage based on histologic examination. Hence, at the processing line myodegenerative changes in the p. major muscle similar to

Line B may not be detected. Because of the difference in collagen distribution between the lines, further research is needed to evaluate how differences in wooden breast p. major muscle morphology will impact fresh-meat quality and further processing.

Collagen biosynthesis is an extremely complex process. There are close to 30 unique vertebrate collagens with tissue-specific distributions. Skeletal muscle consists of types I and III collagen, both of which are fibrillar in nature. The fibrillar collagens such as types I and III contain a single triple-helical domain consisting of three separate peptide chains. The three chains wrap around each other forming an alpha helix and are linked together by interchain disulfide bonds. Once the collagen molecules are secreted from the cell into the connective tissue spaces, and align into a quarter stagger array, crosslinking between the fibrils takes place, leading to fiber formation.

Collagen crosslinking is a progressive process and is associated with the toughing of meat. Muscles with more crosslinking are tougher. The hydroxylsylpyridinoline (HP) crosslink is a mature, nonreducible, trivalent crosslink which results from the condensation of two reducible divalent keto-imine crosslinks (26). Excessive HP crosslinking is associated with the tight parallel packing of collagen as observed in Line A (36). The potential high levels of HP crosslinking in Line A are supported by higher levels of decorin expression in this line. Decorin is an extracellular small leucine-rich repeat proteoglycan and its core protein binds to fibrillar collagens every 67 nm (36) regulating collagen crosslink formation. The necessity of decorin in stabilizing the collagen fibril structure was demonstrated by Danielson et al. (7) in a decorin-deficient mouse. The lack of decorin destabilized the collagen structure due to abnormal collagen crosslinking, leading to skin fragility caused by an abnormal collagen fibrillar network. The significantly higher expression of decorin in the wooden breast–affected Line A p. major muscle supports the increased collagen crosslinking present in this line. Taken together, these data suggest that connective tissue fibrosis associated with the wooden breast myopathy can vary in severity, collagen fiber crosslink formation, distribution of collagen in the extracellular matrix, and effect on breast-meat quality.

To summarize, the wooden breast myopathy at the morphologic level is characterized by muscle fiber necrosis, fibrosis, and muscle fiber regeneration. Gene expression analysis suggests in some lines of broilers that the wooden breast condition can result in excessive collagen crosslinking from very high levels of decorin. Danielson et al. (7) showed in decorin knockout mice that decorin regulates collagen crosslinking and fibrillar structure. The current study represents the first published report comparing the wooden breast condition in three commercial broiler lines, and results from this initial research are suggestive of different cellular mechanisms being evoked. Future research should address the etiology of the wooden breast myopathy as well as investigate cellular mechanisms leading to the muscle degeneration and fibrosis.

REFERENCES

1. Allen, R. E., R. A. Merkel, and R. B. Young. Cellular aspects of muscle growth: myogenic cell differentiation. J. Anim. Sci. 49:115–127. 1979.

2. Bandman, E. Myosin isoenzyme transitions in muscle development, maturation, and disease. Int. Rev. Cytol. 97:97–131. 1985.

3. Bandman, E., R. Matsuda, and R. C. Strohman. Developmental appearance of myosin heavy and light chain isoforms in vivo and in vitro in chicken skeletal muscle. Dev. Biol. 93:508–518. 1982.

4. Brandan, E., C. Cabello-Verrugio, and C. Vial. Novel regulatory mechanisms for proteoglycans decorin and biglycan during muscle formation and muscular dystrophy. Matrix Biol. 27:700–708. 2008.

5. Cooper, R. N., S. Tajbakhsh, V. Mouly, G. Cossu, M. Buckingham, and G. S. Butler-Browne. In vivo satellite cell activation via Myf5 and MyoD in regenerating mouse skeletal muscle. J. Cell Sci. 112:2895–2901. 1999.

6. Cornelison, D. D., and B. J. Wold. 1997. Single-cell analysis of regulatory gene expression in quiescent and activated mouse skeletal muscle satellite cells. Dev. Biol. 191:270–283. 1997.

7. Danielson, K. G., H. Baribault, D. F. Holmes, H. Graham, K. E. Kadler, and R. V. Iozzo. Targeted disruption of decorin leads to abnormal collagen fibril morphology and skin fragility. J. Cell Biol. 136:729–743. 1997.

8. De Luca, A., M. Santra, A. Baldi, A. Giordano, and R. V. Iozzo. Decorin-induced growth suppression is associated with up-regulation of p21, an inhibitor of cyclin-dependent kinases. J. Biol. Chem. 271:18961–18965. 1996.

9. Dransfield, E., and A. A. Sosnicki. Relationship between muscle growth and poultry meat quality. Poult. Sci. 78:743–746. 1999.

10. Goldoni, S., D. G. Seidler, J. Heath, M. Fassan, R. Baffa, M. L. Thakur, R. T. Owens, D. J. McQuillan, and R. V. Iozzo. An antimetastatic role for decorin in breast cancer. Am. J. Pathol. 173:844–855. 2008.

11. Hawke, T. J., and D. J. Garry. Myogenic satellite cells: physiology to molecular biology. J. Appl. Physiol. 91:534–551. 2001.

12. Henke, A., O. C. Grace, G. R. Ashley, G. D. Stewart, A. C. Riddick, H. Yeun, M. O'Donnell, R. A. Anderson, and A. A. Thomson. Stromal expression of decorin, semaphorin6D, SPARC, sprouty1 and tsukushi in developing prostate and decreased levels of decorin in prostate cancer. PLoS One 7:e42516. 2012.

13. Iozzo, R. V. The biology of the small leucine-rich proteoglycans. Functional network of interactive proteins. J. Biol. Chem. 274:18843–18846. 1999.

14. Jarrold, B. B., W. L. Bacon, and A. G. Velleman. Expression and localization of the proteoglycan decorin during the progression of cholesterol induced atherosclerosis in Japanese quail: implications for interaction with collagen type I and lipoproteins. Atherosclerosis 146:299–308. 1999.

15. Kästner, S., M. C. Elias, A. J. Rivera, and Z. Yablonka-Reuveni. Gene expression patterns of the fibroblast growth factors and their receptors during myogenesis of rat satellite cells. J. Histochem. Cytochem. 48:1079–1096. 2000.

16. Kristensen, I. B., L. Pedersen, T. B. Rø, J. H. Christensen, M. B. Lyng, L. M. Rasmussen, H. J. Ditzel, M. Børset, and N. Abildgarrd. Decorin is down-regulated in multiple myeloma and MGUS bone marrow plasma and inhibits HGF induced myeloma plasma cell viability and migration. Eur. J. Haematol. 91:196–200. 2013.

17. Kuttappan, V. A., H. L. Shivaprasad, D. P. Shaw, B. A. Valentine, B. M. Hargis, F. D. Clark, S. R. McKee, and C. M. Owens. Pathological changes associated with white striping broiler breast muscles. Poult. Sci. 92:331–338. 2013.

18. Liu, C., D. C. McFarland, K. E. Nestor, and S. G. Velleman. Differential expression of membrane-associated heparan sulfate proteoglycans in the skeletal muscle of turkeys with different growth rates. Poult. Sci. 85:422–488. 2006.

19. Maruyama, K., and N. Kanemaki. Myosin isoform expression in skeletal muscles of turkeys at various ages. Poult. Sci. 70:1748–1757. 1991.

20. Mauro, A. Satellite cell of skeletal muscle fibers. J. Biophys. Biochem. Cytol. 9:493–495. 1961.

21. Moscatello, D. K., M. Santra, D. M. Mann, D. J. McQuillan, A. J. Wong, and R. V. Iozzo. Decorin suppresses tumor cell growth by activating the epidermal growth factor receptor. J. Clin. Invest. 101:406–412. 1998.

22. Moss, F. P., and C. P. LeBlond. Satellite cells are the source of nuclei in muscles of growing rats. Anat. Rec. 170:421–435. 1971.

23. Mudalal, S., M. Lorenzi, F. Soglia, C. Cavani, and M. Petracci. Implications of white striping and wooden breast abnormalities on quality traits of raw and marinated chicken meat. Animal 9:728–734. 2015.

24. Reed, C. C., J. Gauldie, and R. V. Iozzo. Suppression of tumorigenicity by adenovirus-mediated gene transfer of decorin. Oncogene 21:3688–3695. 2002.

25. Reed, C. C., A. Waterhouse, S. Kirby, P. Kay, R. T. Owens, D. J. McQuillan, and R. V. Iozzo. Decorin prevents metastatic spreading of breast cancer. Oncogene. 24:1104–1110. 2005.

26. Reiser, J. M., R. J. McCromick, and R. B. Rucker. The enzymatic and non-enzymatic crosslinking of collagen and elastin. FASEB J. 6:2439–2449. 1992.

27. Santra, M., C. C. Reed, and R. V. Iozzo. Decorin binds to a narrow region of the epidermal growth factor (EGF) receptor, partially overlapping but distinct from the EGF-binding epitope. J. Biol. Chem. 277:35671–35681. 2002.

28. Schönherr, E., M. Broszat, E. Brandan, P. Bruckner, and H. Kresse. Decorin core protein fragment Leu155-Val260 interacts with TGF-beta but does not compete for decorin binding to type I collagen. Arch. Biochem. Biophys. 355:241–248. 1998.

29. Sihvo, H.-K., and E. Puolanne. Myodegeneration with fibrosis and regeneration in the pectoralis major muscle of broiler. Vet. Pathol. 51:619–623. 2013.

30. Sosnicki, A. A., and B. W. Wilson. Pathology of turkey skeletal muscle: implications for the poultry industry. Food Struct. 10:317–326. 1991.

31. USDA. 2015. Broiler Market News Report. Livest. Poult, Grain Market News Service, Des Moines, IA. 62:19.

32. Velleman, S. G., J. W. Anderson, C. S. Coy, and K. E. Nestor. Effect of selection fro growth rate on muscle damage during turkey breast muscle development. Poult. Sci. 82:1069–1074. 2003.

33. Velleman, S. G., and D. C. McFarland. Myotube morphology, and the expression and distribution of collagen type I during normal and low score normal avian satellite cell myogenesis. Dev. Growth Differ. 41:153–161. 1999.

34. Velleman, S. G., D. C. McFarland, Z. Li, N. H. Ferrin, R. Whitmoyer, and J. E. Dennis. Alterations in sarcomere structure, collagen organization mitochondrial activity, and protein metabolism in the avian low score normal muscle weakness. Dev. Growth Differ. 39:563–570. 1997.

35. Velleman, S. G., and K. E. Nestor. Inheritance of breast muscle morphology in turkeys at sixteen weeks of age. Poult. Sci. 83:1060–1066. 2004.

36. Velleman, S. G., J. D. Yeager, H. Krider, D. A. Carrino, S. D. Zimmerman, and R. J. McCormick. The avian low score normal muscle weakness alters decorin expression and collagen crosslinking. Connect. Tissue Res. 34:33–39. 1996.

37. Weber, I. T., R. W. Harrison, and R. V. Iozzo. Model structure of decorin and implications for collagen fibrillogenesis. J. Biol. Chem. 271:31767–31770. 1996.

38. Wilson, B. W., P. S. Nieberg, and R. J. Buhr. Turkey muscle growth and focal myopathy. Poult. Sci. 69:1553–1562. 1990.

39. Yablonka-Reuveni, Z., and B. Paterson. MyoD and myogenin expression patterns in cultures of fetal and adult chicken myoblasts. J. Histochem. Cytochem. 49:455–462. 2001.

40. Zhu, J., Y. Li, W. Shen, C. Qiao, F. Ambrosio, M. Lavasani, M. Nozaki, M. F. Branca, and J. Huard. Relationships between transforming growth factor-β1 myostatin and decorin: implications for skeletal muscle fibrosis. J. Biol. Chem. 282:25852–25863. 2007.

ACKNOWLEDGMENTS

We thank Cynthia Coy and Rosario Candelero for technical assistance. Funding from the Poultry Cooperative Research Center to S.G.V. is acknowledged.